



Fermi National Accelerator Laboratory

FERMILAB-TM-2000

The D0 Luminosity Monitor Constant for $\sqrt{s} = 630$ GeV

J. Krane, J. Bantly and D. Owen

*Fermi National Accelerator Laboratory
P.O. Box 500, Batavia, Illinois 60510*

July 1997

Disclaimer

This report was prepared as an account of work sponsored by an agency of the United States Government. Neither the United States Government nor any agency thereof, nor any of their employees, makes any warranty, expressed or implied, or assumes any legal liability or responsibility for the accuracy, completeness, or usefulness of any information, apparatus, product, or process disclosed, or represents that its use would not infringe privately owned rights. Reference herein to any specific commercial product, process, or service by trade name, trademark, manufacturer, or otherwise, does not necessarily constitute or imply its endorsement, recommendation, or favoring by the United States Government or any agency thereof. The views and opinions of authors expressed herein do not necessarily state or reflect those of the United States Government or any agency thereof.

Distribution

Approved for public release; further dissemination unlimited.

The DØ Luminosity Monitor Constant for $\sqrt{s} = 630$ GeV

J. Krane, J. Bantly, D. Owen

Fermilab-TM-2000

DØ Note 3222

May. 12, 1997

Abstract

DØ has calculated the luminosity monitor constant for $\sqrt{s} = 630$ GeV. The inelastic $p\bar{p}$ cross section was interpolated between measurements performed at $\sqrt{s} = 546$ and 1800 GeV. The geometric acceptance, hardware efficiency, and luminosity-dependent corrections are similar to those previously published for the full Tevatron energy. We find a luminosity-weighted value of $\sigma_{L\emptyset} = 32.97 \pm 1.05$ mb, yielding a precision of ± 3.19 %.

1 Introduction

During December of 1995, Fermilab reduced the Tevatron's center of mass energy from 1800 GeV to match the energy of previous particle colliders, $\sqrt{s} = 630$ GeV. As a result, the luminosity monitor constant ($\sigma_{L\emptyset}$) for DØ was recalculated with new values for the Level Ø geometric acceptance, the inelastic $p\bar{p}$ cross-sections, the Level Ø hardware efficiency, and the correction factors for multiple single-diffractive events and beam halo. Because the methods of calculation for $\sigma_{L\emptyset}$ remain largely unchanged from previous determinations [1][2] at $\sqrt{s} = 1800$ GeV, the methods receive brief treatment below except where they differ from earlier work.

The Level Ø detector consists of two arrays of scintillating tiles surrounding the Tevatron beampipe and placed 140 cm from the center of the detector

along the beam axis. These hodoscopes were designed to detect the presence of very forward particles generated by inelastic $p\bar{p}$ collisions. Nearly simultaneous hits in the innermost tiles of Level \emptyset (called “good FAST Z hits”) are used to calculate the instantaneous luminosity. The outermost tiles increase the geometric acceptance of the hodoscopes slightly and “good SLOW Z hits” are used in offline analyses. Further details of the Level \emptyset detector may be found in [3].

The multiple interaction-corrected instantaneous luminosity is given [2] by

$$\mathcal{L} = \frac{-\ln(1 - R_{L\emptyset}\tau)}{\sigma_{L\emptyset}\tau},$$

where $R_{L\emptyset}$ is the FAST Z counting rate, τ is the period between beam crossings, and the luminosity monitor constant is defined as

$$\sigma_{L\emptyset} = \epsilon_{L\emptyset} f_{\text{halo}} f_{\text{MSD}} (\epsilon_{\text{SD}}\sigma_{\text{SD}} + \epsilon_{\text{DD}}\sigma_{\text{DD}} + \epsilon_{\text{HC}}\sigma_{\text{HC}}).$$

Here, the inelastic $p\bar{p}$ cross section has been split into three components (single diffractive, double diffractive, and hard-core) because the geometric acceptance (ϵ_i) for each process differs greatly. While the halo and multiple single diffractive correction factors (f_{halo} and f_{MSD}) are negligibly close to unity in the range of low luminosities experienced during the low-energy run, they are included in the calculation for completeness and consistency with prior determinations. Finally, the hardware efficiency ($\epsilon_{L\emptyset}$) was calculated as a constant with respect to luminosity due to the limited luminosity range. The luminosity monitor constant may be interpreted as the portion of the inelastic cross section observable to the D \emptyset detector, thus $\sigma_{L\emptyset}$ is sometimes called the Level \emptyset visible cross section.

2 Calculation of cross section values

Calculation of the Level \emptyset cross section requires a measurement of the single diffractive, elastic, and total cross sections (σ_{SD} , σ_{EL} , and σ_{TOT}) at the intended center of mass energy. For $\sqrt{s} = 1800$ GeV, the world average cross section values were computed using published data from CDF [4] and E710 [5]. Because the results of the two experiments do not agree well, the uncertainty on the average value was increased by a factor of χ as described in Reference [1].

A complete set of three cross sections does not exist at $\sqrt{s} = 630$ GeV. The nearest complete set of measurements were performed at a center-of-mass energy of 546 GeV [4][6][7]. This section details the methodology used to interpolate the cross section values between 546 and 1800 for use at 630 GeV.

In the literature [7][8] the total $p\bar{p}$ cross section is expected to follow a $\ln^2 s$ dependence. In contrast, the elastic and single diffractive cross sections obey an observed $\ln s$ dependence [9]. A two parameter form ($a \ln^n s + b$) was used to interpolate each cross section, where n had a value of 2 to fit the total cross section and 1 otherwise. Because the target point of the interpolation is very close to one end-point of the fit, the error at 630 GeV is largely driven by the error at 546 GeV. Figure 1 displays the results of the fits. Table 1 lists the fit parameters a and b , the uncertainty on the parameters, and the covariance between a and b for the three cross sections. Table 2 summarizes the values and uncertainties found for σ_{SD} , σ_{EL} , and σ_{TOT} at $\sqrt{s} = 630$ GeV.

	a	b	$\text{Cov}(a, b)$
σ_{TOT}	0.2447 ± 0.0535	22.554 ± 8.711	-0.464
σ_{EL}	2.541 ± 0.545	-19.070 ± 6.992	-3.84
σ_{SD}	0.538 ± 0.413	1.471 ± 6.010	-2.48

Table 1: Fit parameters, errors and covariance.

σ_{TOT}	63.223 ± 0.829 mb
σ_{EL}	13.683 ± 0.290 mb
σ_{SD}	8.432 ± 0.641 mb

Table 2: Calculated cross sections and uncertainties at $\sqrt{s} = 630$ GeV.

The fit to the total cross section was compared to the result obtained by the UA4/2 Collaboration [8] using a more complicated 8 parameter fit. UA4/2 modeled the \sqrt{s} evolution of the total $p\bar{p}$ cross section from 5 to 546 GeV with dispersion relations and 103 data points. They extrapolated their best fit to all data to LHC and SSC energies; their intermediate points are shown in Figure 2. The UA4/2 best fit points at 546, 900, and 1800 GeV are in excellent agreement with the simpler fit to the total cross section used

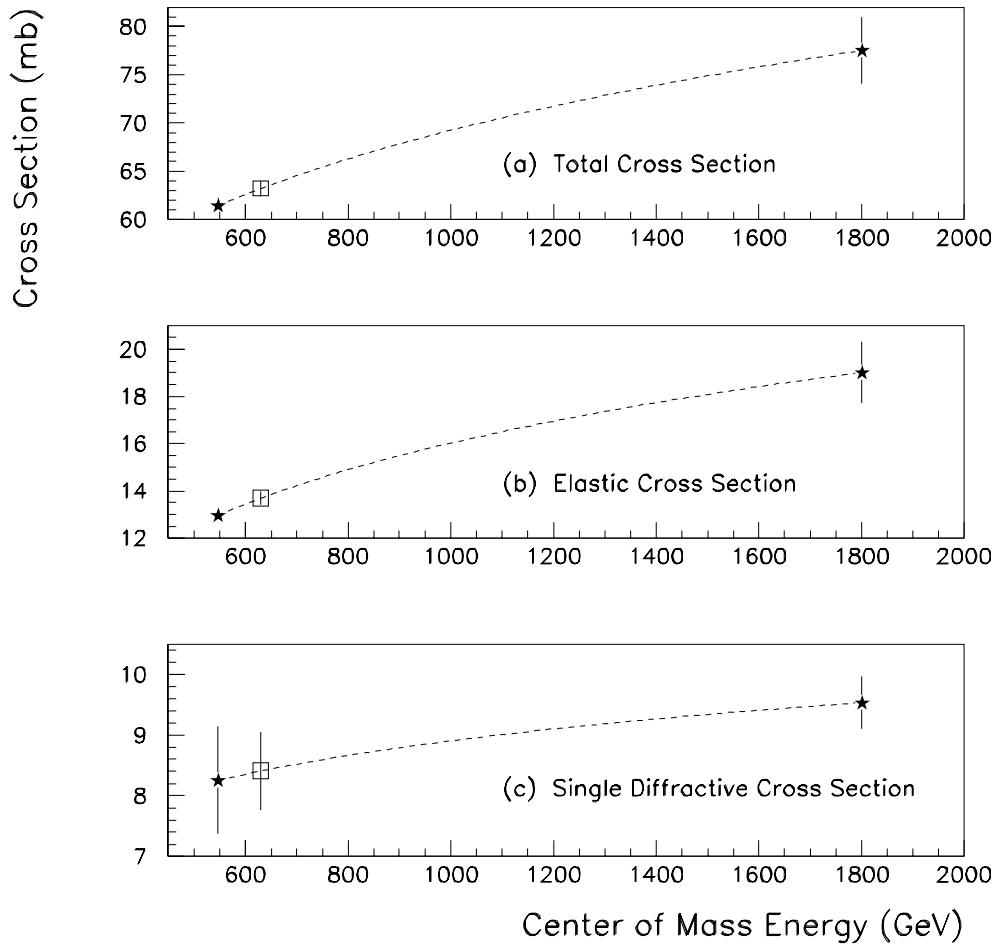


Figure 1: The results of interpolation for the (a) total, (b) elastic, and (c) single diffractive $p\bar{p}$ cross sections. The stars denote the world average cross sections at 546 and 1800 GeV, while the squares indicate the interpolated points at $\sqrt{s} = 630$ GeV. The dashed line represents the two parameter fit.

for the $\sigma_{L\emptyset}$ calculation. To estimate the uncertainty of interpolation due to the simple functional form of the model used in the $\sigma_{L\emptyset}$ calculation, the variance between the UA4/2 extrapolation and the simple interpolation (0.23%) is included as an error in quadrature with the other fitting uncertainties.

As detailed in reference [1], the double-diffractive and hard-core components of the $p\bar{p}$ cross section are calculated from the world average cross sections. The resulting values are presented in Table 3.

σ_{SD}	8.432 ± 0.641 mb
σ_{DD}	1.299 ± 0.238 mb
σ_{HC}	39.810 ± 1.113 mb

Table 3: The calculated components of the inelastic $p\bar{p}$ cross section.

3 Geometric Acceptance of Level \emptyset

Monte Carlo studies determine the acceptance of the Level \emptyset hodoscopes by calculating the probability that one or more charged particles will pass through the scintillating tiles. The probabilities were calculated with MBR [4] and DTUJet [10], two minbias event generators. Samples of 6000 events each were generated for each of the three inelastic processes and passed through D \emptyset GEANT [11] and D \emptyset RECO (the D \emptyset detector simulator and reconstruction algorithms, respectively). The results are summarized in Figure 3. The MBR Monte Carlo program randomly selects a diffracted particle in SD interactions, while DTUJet generates events with either the proton or the antiproton diffracted each time. Some events are “lost” during the GEANT or RECO stage, but the final sample size in each case is nominally 6000 events.

The results indicate a small decrease in acceptance when compared to the results of the $\sqrt{s} = 1800$ GeV study. For each subprocess, the geometric acceptance decreased by 1–3 percent due to lower particle multiplicity at lower center of mass energy.

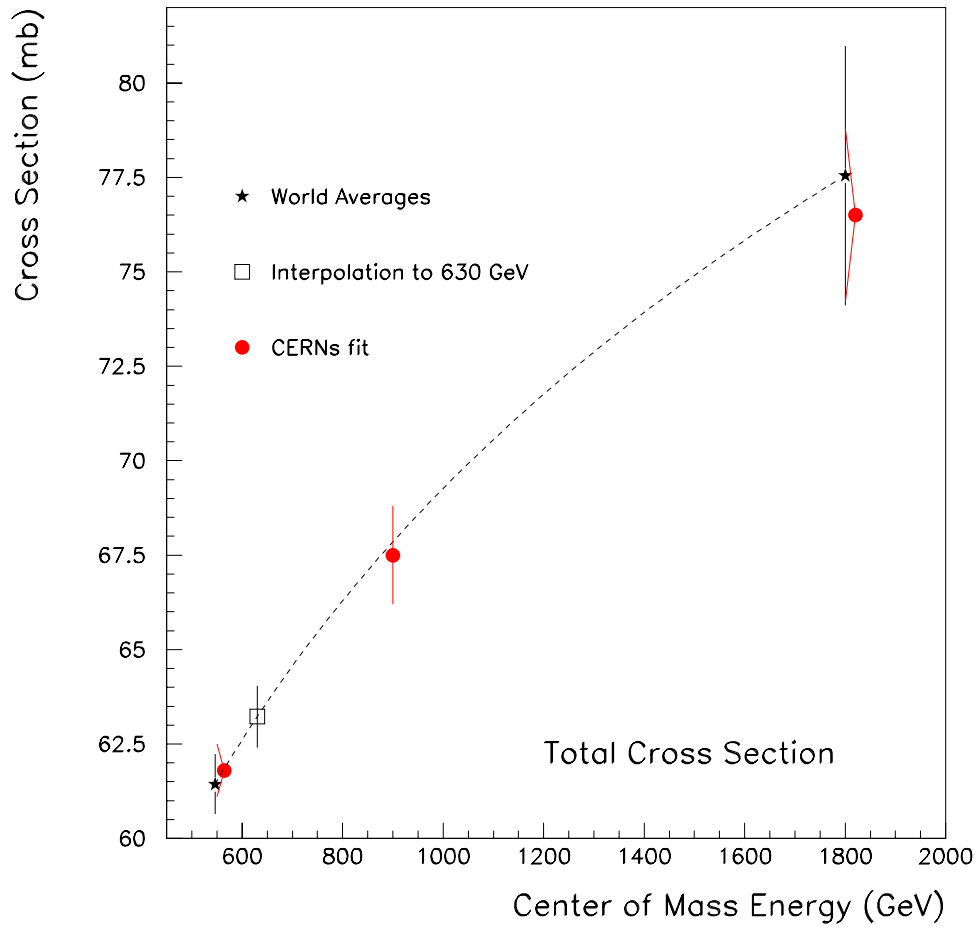


Figure 2: The world average total $p\bar{p}$ cross section at 546 and 1800 GeV (stars), interpolated to 630 GeV (square). The dashed line is the two parameter fit. The points from CERN's UA4/2 Collaboration (circles) are included for comparison.

Final numbers from MBR and DTUJet for Level 0 Acceptance at 630 GeV CM Energy

	TOTAL EVENTS IN SAMPLE	number	good FAST Z percent	stat error
DTUJet				
Single Diffractive, proton diffracted	5997	444	7.40%	0.34%
Single Diffractive, antiproton diffracted	6000	454	7.57%	0.34%
Double Diffractive	5999	4217	70.30%	0.59%
Hard Core	6000	5778	96.30%	0.24%
MBR				
Single Diffractive	5957	1102	18.50%	0.50%
Double Diffractive	5979	3946	66.00%	0.61%
Hard Core	5997	5704	95.11%	0.28%
DTUJet				
		number	good SLOW Z percent	stat error
Single Diffractive, proton diffracted	5997	514	8.57%	0.36%
Single Diffractive, antiproton diffracted	6000	527	8.78%	0.37%
Double Diffractive	5999	4324	72.08%	0.58%
Hard Core	6000	5829	97.15%	0.22%
MBR				
Single Diffractive	5957	1186	19.91%	0.52%
Double Diffractive	5979	4005	66.98%	0.61%
Hard Core	5997	5743	95.77%	0.26%

AVERAGES	FAST Z ACCEPTANCE	SLOW Z ACCEPTANCE
SINGLE DIFFRACTIVE	12.99% \pm 6.95%	14.35% \pm 0.73%
DOUBLE DIFFRACTIVE	68.15% \pm 0.85%	69.53% \pm 0.84%
HARD CORE	95.71% \pm 0.37%	96.46% \pm 0.34%

Figure 3: Summary of geometric acceptance studies. FAST Z indicates the number and percentage of events with at least one particle passing through each Level 0 hodoscope. (The SLOW Z numbers, included for completeness, are germane to data triggers and luminosity studies, but not to the instantaneous luminosity measurement.)

4 Level \emptyset Hardware Efficiency and Luminosity-dependent Effects

4.1 Hardware Efficiency

The method used to evaluate the Level \emptyset hardware efficiency ($\epsilon_{L\emptyset}$) is discussed at length in reference [2]. Briefly, we define hardware efficiency as the per-event acceptance of the Level \emptyset hodoscopes for events with particles that pass through both arrays. It was found that the scintillating tiles were least likely to detect events with very low particle multiplicity, resulting in a small luminosity dependence in $\epsilon_{L\emptyset}$. Because the particle multiplicity of inelastic collisions at $\sqrt{s} = 630$ GeV is smaller than comparable events at 1800 GeV, the observed decrease in hardware efficiency is to be expected.

In Figure 4, the hardware efficiency found at 630 GeV lies approximately seven percent lower than the 1800 GeV points at similar luminosity. No attempt was made to include a luminosity dependence in the 630 number, the single point is used throughout the luminosity range ($1 \cdot 10^{28}$ to $2.6 \cdot 10^{30}$ $\text{cm}^{-2} \cdot \text{sec}^{-1}$).

4.2 Multiple Single Diffractive Events

In Section 3, the calculation of the geometric acceptance assumed all events were single interactions. A single diffractive event has a low probability of firing both Level \emptyset hodoscopes because the trajectory of the non-fragmented particle usually remains within the beampipe. At high luminosities, there is a calculable probability that two (or more) single diffractive events will occur simultaneously but in opposite directions. Such an occurrence mimics a double diffractive event and shares the much higher acceptance. While the expression for the luminosity given previously accounts for multiple interactions, it does so in a simple way that neglects the effect of multiple single diffractive events (MSD).

In high-luminosity environments MSD effects can be significant; during the 630 GeV running period, the effect of MSD was much less pronounced (see Figure 5(a)).

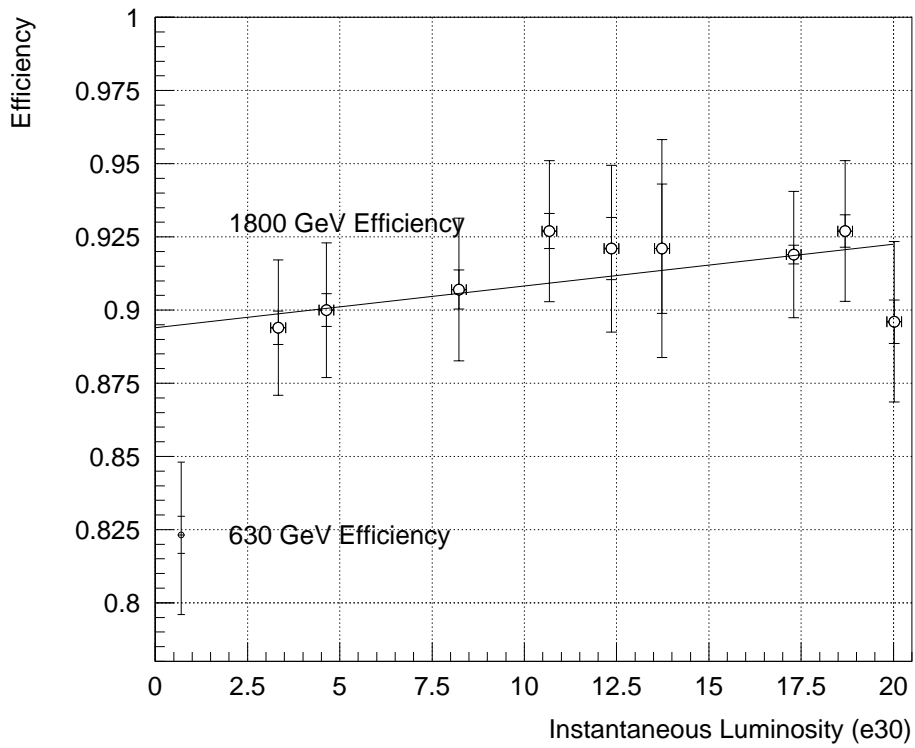


Figure 4: The Level 0 hardware efficiency at $\sqrt{s} = 1800$ and 630 GeV. The residual luminosity dependence is negligible over the luminosity range of the low-energy run ($1 \cdot 10^{28}$ to $3 \cdot 10^{30} \text{ cm}^{-2} \cdot \text{sec}^{-1}$).

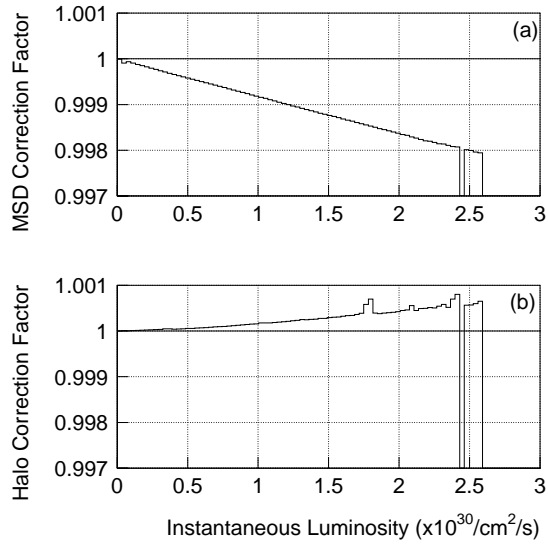


Figure 5: The (a) MSD correction and the (b) Halo correction as functions of instantaneous luminosity. The corrections are each less than 0.2% and partially offset one another. Discontinuities in the halo correction are caused by unusually high halo rates in several isolated runs.

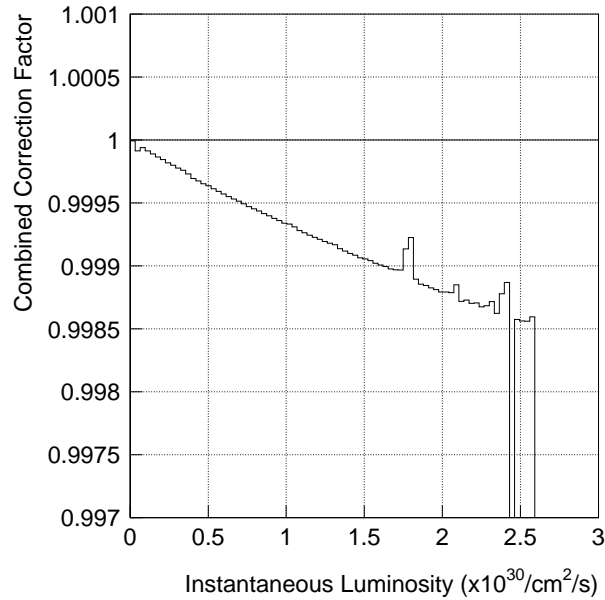


Figure 6: The combined correction factor as a function of instantaneous luminosity. Together, the corrections reach a maximum of 0.15%.

4.3 Beam Halo Correction

Particle orbits within the Tevatron do not always follow a simple closed path. Particles with a trajectory some transverse distance from the nominal bunch center follow an orbit that oscillates about the closed path. The amplitude of these oscillations tends to grow during the course of a store, eventually resulting in collisions with beampipe hardware [12]. The resulting particle cascades can pass through detectors and distort physics measurements. For this reason, “halo events” are rejected at the trigger level, with the unfortunate consequence of distorting luminosity measurements. The correction derived from measured halo rates is shown as a function of instantaneous luminosity in Figure 5(b). (The effect of beam halo depends on both beam characteristics and luminosity, thus varying from run to run as highlighted by the discontinuities in Figure 5(b). While the correction is applied on a run-to-run basis the correction is best viewed as a function of the stronger luminosity-dependence.) The combined MSD and halo corrections are listed in Figure 6. The effect at all instantaneous luminosities is less than 0.15%.

5 Summary

DØ has calculated the luminosity monitor constant for $\sqrt{s} = 630$ GeV, considering changes in efficiency due to lower $p\bar{p}$ inelastic cross sections, differing particle kinematics, and luminosity-dependent considerations. The small run-dependent halo effect was included and the hardware efficiency of the scintillating hodoscopes was remeasured. A numeric interpolation of $p\bar{p}$ cross sections between $\sqrt{s} = 546$ and 1800 GeV was performed because no direct measurements are available. We find a final luminosity-weighted average $\sigma_{L\text{Ø}} = 32.97 \pm 1.05$ mb, a fractional uncertainty of ± 0.0319 .

The results of the individual components of the calculation are listed in Table 4 with the final result. Note that only the central values are listed, the MSD and beam halo corrections do vary slightly with instantaneous luminosity.

$\epsilon_{SD}\sigma_{SD} + \epsilon_{DD}\sigma_{DD} + \epsilon_{HC}\sigma_{HC}$	40.081 ± 1.282 mb
$\epsilon_{L\emptyset}$	0.8232 ± 0.0257
$f_{\text{halo}} \cdot f_{\text{MSD}}$	0.99924 ± 0.00200
$\sigma_{L\emptyset}$	32.97 ± 1.05 mb

Table 4: Results for the calculation of the luminosity monitor constant for $\sqrt{s} = 630$ GeV.

We thank the staffs at Fermilab and the collaborating institutions for their contributions to this work, and acknowledge support from the Department of Energy and National Science Foundation (U.S.A.), Commissariat à l’Energie Atomique (France), State Committee for Science and Technology and Ministry for Atomic Energy (Russia), CNPq (Brazil), Departments of Atomic Energy and Science and Education (India), Colciencias (Colombia), CONACyT (Mexico), Ministry of Education and KOSEF (Korea), CONICET and UBACyT (Argentina), and the A.P. Sloan Foundation.

References

- [1] J.Bantly, A.Brandt, R.Partridge, J.Perkins, D.Puseljic, *Improvement to the $D\emptyset$ Luminosity Monitor Constant*, Fermilab Tech. Memo. TM-1930, 1995.
- [2] J.Bantly, J.Krane, D.Owen, R.Partridge, L.Paterno, *$D\emptyset$ Luminosity Monitor Constant for the 1994-1996 Tevatron Run*, Fermilab Tech. Memo. TM-1995, 1 Feb. 1997.
- [3] J.Bantly, K.Epstein, J.Fowler, G.S.Gao, R.Hlustick, R.E.Lanou, F.Nang, R.Partridge, L.Wang, and H.Xu, *IEEE Trans. on Nucl. Sci.* **41**, 1274 (1994).
- [4] F. Abe et al., the CDF Collaboration, “Measurement of the $p\bar{p}$ Total Cross Section at $\sqrt{s} = 546$ and 1800 GeV”, *Phys. Rev. D* **50** (1994) 5550.
- [5] N. Amos et al., “A Luminosity Independent Measurement of the $p\bar{p}$ Total Cross Section at $\sqrt{s} = 1.8$ TeV”, *Phys. Lett. B* **242**, 158 (1990).

- [6] D. Bernard, et al., the UA4 Collaboration, “The Cross Section of Diffraction Dissociation at the CERN SPS Collider”, Phys. Lett. B, 186, 2, March 5, 1987.
- [7] M. Bozzo, et al., “Measurement of the Proton-Antiproton Total and Elastic Cross Sections at the CERN SPS Collider”, the UA4 Collaboration, Phys. Lett. 147B, number 4, 5, November 8, 1984.
- [8] C. Augier, et al., UA4/2 Collaboration, “Predictions on the total cross section and real part at LHC and SSC”, Phys. Lett. B315, pp. 503-506, 1993.
- [9] G. Chiarelli, for the CDF Collaboration, “Measurement of $p\bar{p}$ Elastic and Total Cross Section at $\sqrt{s} = 546$ and 1800 GeV at CDF”, FERMILAB-Conf-93/360-E.
- [10] P.Aurenche, *et al.*, Phys. Rev. **D45** (1992) 92. See also, F.W.Bopp, *et al.*, Z. Phys. **C51** (1991) 99.
- [11] A.Jonckheere, “Proceedings of the Argonne National Laboratory Detector Simulation Workshop”, August 1987. See also F.Carminati, *et al.*, “GEANT User’s Guide”, CERN Program Library (Dec 1991).
- [12] Private correspondence with John Marriner, Beams Division, Fermilab.